Human Molecular Genetics, 2006, Vol. 15, No. 9 ***1437–1449***
doi:10.1093/hmg/ddl066
Advance Access published on March 21, 2006

Mitochondria are a direct site of Aβ accumulation in Alzheimer's disease neurons: implications for free radical generation and oxidative damage in disease progression

Maria Manczak[1], Thimmappa S. Anekonda[1], Edward Henson[2], Byung S. Park[3], Joseph Quinn[2] and P. Hemachandra Reddy[1,*]

[1]Neurogenetics Laboratory, Neurological Sciences Institute, Oregon Health and Science University, 505 NW 185th Avenue, Beaverton, OR 97006, USA, [2]Department of Neurology and [3]Division of Biostatistics, Department of Public Health and Preventive Medicine, Oregon Health and Science University, 3181 S.W. Sam Jackson Park Road, Portland, OR 97201, USA

Received February 5, 2006; Revised and Accepted March 14, 2006

Alzheimer's disease (AD) is a complex, neurodegenerative disease characterized by the impairment of cognitive function in elderly individuals. In a recent global gene expression study of APP transgenic mice, we found elevated expression of mitochondrial genes, which we hypothesize represents a compensatory response because of mitochondrial oxidative damage caused by the over-expression of mutant APP and/or amyloid beta (Aβ). We investigated this hypothesis in a series of experiments examining what forms of APP and Aβ localize to the mitochondria, and whether the presence of these species is associated with mitochondrial dysfunction and oxidative damage. Using immunoblotting, digitonin fractionation, immunofluorescence, and electron microscopy techniques, we found a relationship between mutant APP derivatives and mitochondria in brain slices from Tg2576 mice and in mouse neuroblastoma cells expressing mutant human APP. Further, to determine the functional relationship between mutant APP/Aβ and oxidative damage, we quantified Aβ levels, hydrogen peroxide production, cytochrome oxidase activity and carbonyl proteins in Tg2576 mice and age-matched wild-type (WT) littermates. Hydrogen peroxide levels were found to be significantly increased in Tg2576 mice when compared with age-matched WT littermates and directly correlated with levels of soluble Aβ in Tg2576 mice, suggesting that soluble Aβ may be responsible for the production of hydrogen peroxide in AD progression in Tg2576 mice. Cytochrome *c* oxidase activity was found to be decreased in Tg2576 mice when compared with age-matched WT littermates, suggesting that mutant APP and soluble Aβ impair mitochondrial metabolism in AD development and progression. An increase in hydrogen peroxide and a decrease in cytochrome oxidase activity were found in young Tg2576 mice, prior to the appearance of Aβ plaques. These findings suggest that early mitochondrially targeted therapeutic interventions may be effective in delaying AD progression in elderly individuals and in treating AD patients.

INTRODUCTION

Alzheimer's Disease (AD) is a complex, heterogeneous and progressive dementia that is associated with neurofibrillary tangles and amyloid beta (Aβ) plaques (1–4). Neurofibrillary tangles and Aβ deposits have been found primarily in the regions of memory and cognition in AD patients and in AD transgenic mice. Since the discovery of the 4 kDa Aβ peptide—a cleaved product of amyloid precursor protein (APP) via sequential proteolysis of aspartyl beta secretase

*To whom correspondence should be addressed. Tel: +1 5034182625; Fax: +1 5034182501; Email: reddyh@ohsu.edu

and presenilin-dependent secretase in AD brains—much research has focused on understanding Aβ toxicity and its relationship with AD progression and pathogenesis (5–7). It is now generally accepted that a progressive accumulation of Aβ aggregates eventually triggers a cascade of cellular changes, including mitochondrial oxidative damage, the hyperphosporylation of tau, synaptic failure and inflammation (8–18). However, initial triggers of mutant APP and/or intracellular Aβ are not clearly understood.

To understand the early and progressive cellular changes in AD development and progression, using cDNA microarray techniques, our laboratory recently investigated mRNA expressions in an AD transgenic mouse model (Tg2576) at three stages of disease progression: long before (2-months old), immediately before (5-months old) and after (18-months old), the appearance of amyloid pathology and cognitive impairment. A comparative gene expression analysis of Tg2576 mice and age-matched wild-type (WT) littermates (control) revealed that genes related to mitochondrial energy metabolism and apoptosis were up-regulated in the 2-, 5- and 18-month-old Tg2576 mice compared with the genes in WT littermates. These results suggest that, in the progression of AD, mitochondrial energy metabolism may be impaired by the expression of mutant APP, and/or soluble and insoluble Aβ (14).

The impairment of mitochondrial metabolism in AD patients has been well documented in the literature of AD (11–13,19–24). In addition, several *in vitro* studies of Aβ and mitochondrial function have reported that Aβ affects mitochondrial DNA and proteins, leading to impairments of the electronic transport chain (ETC) and ultimately mitochondrial dysfunction (9,10,23–31). Recently, Lustbader *et al.* (32) reported that Aβ-binding alcohol dehydrogenase directly interacts with Aβ in the mitochondria of AD patients and transgenic mice and that this interaction promotes the leakage of reactive oxygen species, ultimately leading to mitochondrial dysfunction. Markers of oxidative stress, including the oxidation of proteins, were found in AD brains (33). Further, the oxidation of DNA (9,10) and proteins (22,34) were found to be increased in Tg2576 mice compared with those in age-matched WT mice, suggesting that oxidative damage in the AD brain contributes to AD pathogenesis before Aβ accumulates (22,33,34). Evidence of abnormal mitochondrial gene expressions from our gene expression studies (14) suggests that mutant APP or Aβ may affect mitochondrial function, which, in turn, may generate reactive oxygen species, ultimately leading to oxidative damage in AD. If this hypothesized chain of events is confirmed, our gene expression data showing the up-regulation of mitochondrial genes may be interpreted as a compensatory response to mitochondrial dysfunction induced by mutant APP or Aβ (14). However, it is unclear how mitochondrial genes in Tg2576 mice are activated even before plaque formation—particularly in amyloid-rich regions of the Tg2576 mouse brain, and it is unclear whether Aβ is localized to mitochondria, whether this localization leads to impairment of the ETC, and whether, ultimately, these impairments induce free radicals. It is also unclear whether Aβ1–40 or Aβ1–42, or both, affect mitochondrial function.

To address these issues, in the present study, using biochemical and molecular methods, we studied the localization of Aβ in the mitochondria of Tg2576 mice and also in stably expressed mutant APP (Swe) in neuroblastoma (N2a) cell lines (35). We also measured soluble and insoluble Aβ1–40 and Aβ1–42 in the amyloid-rich region (the cerebral cortex) of 2-, 12- and 17-month-old Tg2576 mice. To determine whether Aβ1–40 and/or Aβ1–42 directly influences mitochondrial function, we measured hydrogen peroxide levels and cytochrome *c* oxidase activity in Tg2576 mice and in age-matched WT littermates (control). To determine the relationship between mutant APP, Aβ and oxidative damage, we used immunofluorescence methods to study 8-hydroxyguanosine (8-OHG; an oxidative damage marker) and Aβ immunoreactivity in the 2-, 8- and 17-month-old Tg2576 mice and age-matched WT littermates (control).

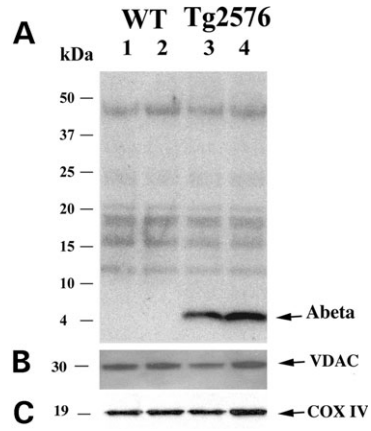

Figure 1. Immunoblotting analysis of Aβ in cortical mitochondria of Tg2576 mice. Ten μg of mitochondrial protein lysate was used from each sample, and immunoblotting analysis was carried out using an Aβ1–40 antibody. To detect 4 kDa Aβ peptides, mitochondrial protein lysates were run on a 10–20% gradient Tricine/SDS gel. No 4 kDa Aβ monomers were found in the WT mice (lanes 1 and 2), but they were detected in the Tg2576 mice (lanes 3 and 4) and in the 4 kDa band (**A**). Bottom panel represents immunoreactivities of VDAC (**B**) and COX IV (**C**) after strip elution of the same membrane immunoblotted with the Aβ1–40 antibody.

RESULTS

Evidence from Tg2576 mice: association between Aβ1–40, Aβ1–42 and mitochondria

To determine whether there is a relationship between Aβ and mitochondria, immunoblotting analysis was performed on isolated mitochondria from 6-month-old Tg2576 mice and age-matched WT mice. As shown in Figure 1, a 4 kDa Aβ monomer was detected only in the Tg2576 mice (lanes 3 and 4), and the 4 kDa band was completely absent in the WT mice, suggesting that 4 kDa Aβ is associated with mitochondria. To determine whether the 4 kDa Aβ is part of Aβ1–40 (the shorter form) or Aβ1–42 (the longer form), or both, we ran the mitochondrial protein lysates in a 4–20% gradient gel. As shown in Figure 2, a doublet of Aβ1–40 and Aβ1–42 bands were found in isolated mitochondria from the cortical tissues of the Tg2576 mice but not in the age-matched WT mice, suggesting that both Aβ1–40 and Aβ1–42 are associated with mitochondria.

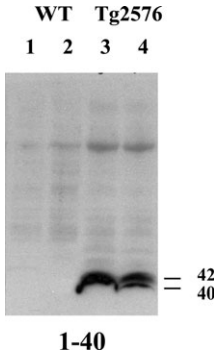

Figure 2. Immunoblotting analysis of Aβ in cortical mitochondria of Tg2576 mice and age-matched WT littermates. Ten μg of a mitochondrial protein lysate was taken from each cortical sample, and immunoblotting analysis was carried out using an Aβ1–42 antibody. To determine whether the 4 kDa monomer is a part of Aβ1–40 or Aβ1–42, or both, we ran the protein lysates in a 4–20% gradient gel using standard western blotting conditions and an Aβ1–42 polyclonal antibody. A doublet of Aβ1–40 and Aβ1–42 bands was found in the mitochondria isolated from the cortical tissues of Tg2576 mice, but not in the mitochondria isolated from age-matched WT mice.

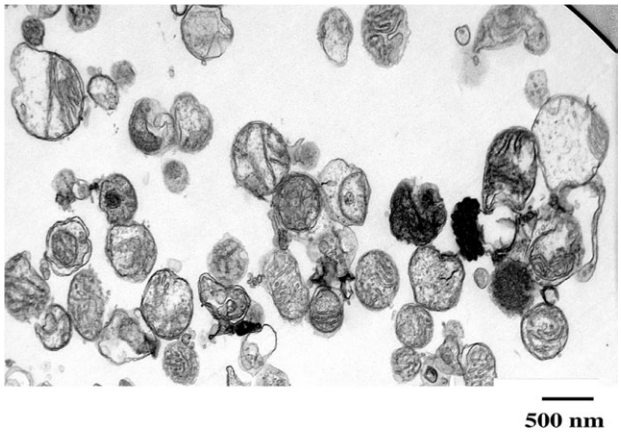

Figure 3. Electron microscopy of isolated mitochondria from Tg2576 mice. To determine the purity of the mitochondrial pellets used in this study, we isolated mitochondria from Tg2576 mice and age-matched WT littermates, fixed them in Karnovsky's fixative, and embedded them in Epon 812 at 60°C for 12 h. Blocks were sectioned on a Leica Ultramicrotome, and sections were viewed on an FEI Morgagni electron microscope.

To ensure the purity of the mitochondrial preparation from the cortical tissues of the Tg2576 and WT mice, we performed electron microscopy using mitochondrial pellets. As shown in Figure 3 and Supplementary Material, Figure S1, these mitochondrial preparations showed an enrichment of mitochondria (over 90%); rarely did we find lysosomes in the mitochondrial preparation.

Evidence from APP cell lines: oligomeric forms of Aβ are associated with mitochondria; Aβ is localized to the inner mitochondrial membrane

To confirm a relationship between Aβ and mitochondria, we studied Aβ and mitochondrial association in another

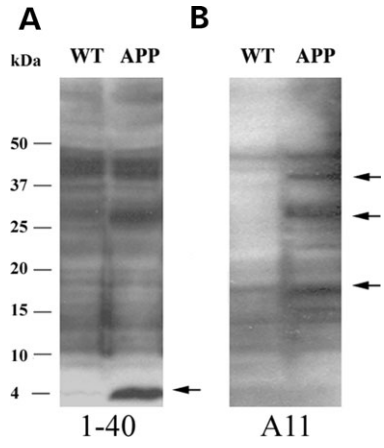

Figure 4. Immunoblotting analysis of Aβ in mitochondria from mutant human APP and WT human APP stably expressed in N2a cell lines. Ten μg of mitochondrial protein lysate was loaded from each sample, and immunoblotting analysis was carried out using a 1–40 polyclonal antibody (**A**) and an A11-oligomer antibody (**B**). The 4 kDa monomer was enriched in N2a cells expressed with mutant APP (**A**), but not in WT APP expressed in N2a cells (**B**). Oligomer Aβ bands of differing sizes were present only in mutant APP cells.

system: mouse N2a cells stably expressing human mutant APP and human WT APP. This immunoblotting analysis showed 4 kDa Aβ in isolated mitochondria from mutant APP cell lines, but not in the mitochondrial pellet from WT APP cells, supporting the relationship between Aβ and mitochondria that we found in the Tg2576 mice (Fig. 4A). Further, to determine whether an oligomer formation of Aβ is also associated with mitochondria, we conducted immunoblotting analysis using an A11 antibody (which recognizes oligomers but not monomers) (36). As shown in Figure 4B, we found three distinct bands, ranging from 15 to 50 kDa of oligomers only in the mitochondrial pellet from the mutant APP cells, not in the mitochondrial pellet from the WT cells, suggesting that both monomers and oligomers of Aβ are associated with mitochondria.

To determine whether oligomer formation of Aβ is associated with a mitochondrial extract, we carried out immunoblotting analysis using (a) protein lysates from nuclear and mitochondrial extracts and (b) an A11-oligomer antibody that recognizes only oligomers. As shown in Figure 5, in mutant APP cell lines, we found oligomer formations mainly in the mitochondrial extract, less abundantly in the nuclear extract of mutant cells, and not in the nuclear extracts of cells expressing human WT APP. However, we found traces of oligomer formation in mitochondrial extracts of cells expressing human WT APP. These results demonstrated that both monomer and oligomers of Aβ are associated with mitochondria, suggesting that Aβ may likely localize to mitochondria and possibly cause mitochondrial dysfunction.

To determine whether Aβ is localized to mitochondria, in particular to the outer membrane or mitoplast (inner membrane plus matrix), we further dissected Aβ in association with mitochondria, using a digitonin-fractionation method (37) and immunoblotting analysis. Our immunoblotting

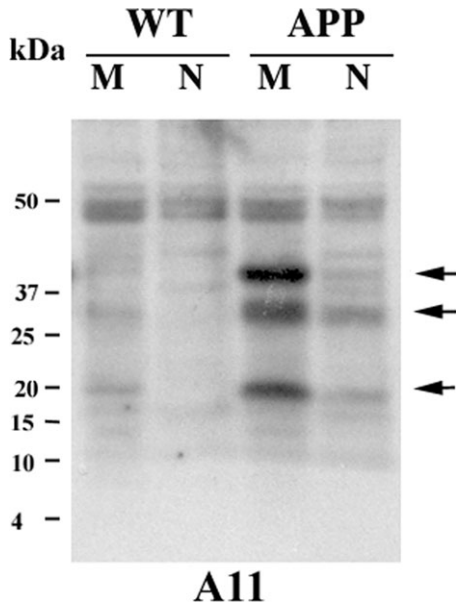

Figure 5. Immunoblotting analysis of Aβ in mitochondria from mutant human APP and WT human APP stably expressed in N2a cell lines. Ten μg of nuclear and mitochondrial protein lysates were loaded from the cell-lines, and immunoblotting analysis was carried out using an A11 antibody (36) specific for oligomer Aβ. Oligomers were found mainly in the mitochondrial pellet of the mutant human APP cell line, not in that of the WT human APP cell line.

analysis of digitonin-fractionated mitochondrial membranes revealed that most of the Aβ was in the mitoplast fraction and some was in the outer membrane of mitochondria, suggesting that Aβ enters mitochondria and localizes to mitoplast (Fig. 6). Further, using immunoblotting analyses of several antibodies specific to mitochondria, including Mn-SOD (matrix), COX IV and adenine nucleotide translocator (ANT; inner membrane), we further confirmed that Aβ is primarily localized to the mitoplast (inner membrane plus matrix). The immunoreactivity of Mn-SOD (matrix), COX IV and ANT were robust in lane 2 (Fig. 6) containing the mitoplast fraction and not in lane 3 (Fig. 6) containing the outer mitochondrial membrane fraction.

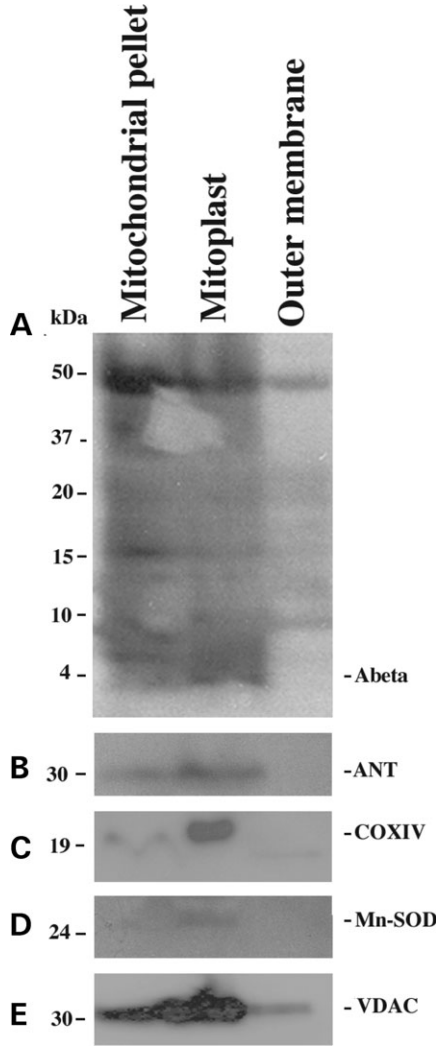

Figure 6. Immunoblotting analysis of Aβ in digitonin-fractionated mitochondria from mutant APP. Five μg of mitochondrial membranes was resolved in a 10–20% Tricine–SDS gel, and immunoblotting analysis was carried out using a 1–40 polyclonal antibody. (**A**) Aβ was found in abundance in the mitochondrial fraction containing the inner mitochondrial membrane and the mitochondrial matrix (lane 2), and less abundantly in the outer mitochondrial membrane (lane 3). (**B**) represents the immunoreactivity of ANT (inner membrane protein) after strip elution of the same membrane used in (A). ANT was found in lanes 1 (total mitochondria) and 2 (mitopalst, inner membrane plus matrix), but was absent in lane 3 (outer mitochondrial membrane). (**C**) represents the immunoreactivity of COXIV. COXIV was found in lanes 1 (total mitochondria) and 2 (inner membrane plus matrix). (**D**) represents Mn-SOD, and was found in lanes 1 (total mitochondria) and 2 (inner membrane plus matrix), but was absent in lane 3 (outer mitochondrial membrane). (**E**) represents the immunoreactivity of VDAC after strip elution of the same membrane immunoblotted with the Aβ antibody. VDAC is an outer mitochondrial membrane protein. However, VDAC is abundant in inner- and outer-mitochondrial membrane contact sites (57,58). VDAC immunoreactivity was found in lanes 1 (total mitochondrial pellet), 2 (inner membrane plus matrix) and 3 (outer mitochondrial membrane).

Intraneuronal Aβ and Aβ deposits in Tg2576 mice

To determine the time course of mutant APP expression and of Aβ formation, using immunohistochemical methods, we investigated cerebral cortex and hippocampus slices from 2-, 8- and 17-month-old Tg2576 mice. Our immunofluorescence analysis revealed no Aβ deposits in the 2-month-old Tg2576 mice, very few in the 8-month-old Tg2576 mice (data not shown) and an abundance in the 17-month-old Tg2576 mice (Fig. 8). As shown in Figure 8, we found intraneuronal Aβ in the 2-month-old Tg2576 mice, and the numbers progressively increased in an age-dependent manner to the 17-month-old Tg2576 mice. In addition, using ELISA, we also measured both soluble and insoluble Aβ levels in Tg2576 mice at three stages of disease progression (2-, 12- and 17-months old (Table 1). In the 2-month-old Tg2576 mice, we detected both soluble Aβ1–40 and Aβ1–42 intraneuronally, but no insoluble Aβ. In the 12-month-old Tg2576 mice, we found both soluble and insoluble Aβ, and in the 17-month-old Tg2576 mice, we found increased levels of both soluble and insoluble Aβ.

Table 1. Summary of age-dependent Aβ levels in Tg2576 mice

	Number of Tg2576 mice	Sol Aβ1–40 Mean ± SE (pg Aβ/mg protein)	Insol Aβ1–40 Mean ± SE (pg Aβ/mg protein)	Sol Aβ1–42 Mean ± SE (pg Aβ/mg protein)	Insol Aβ1–42 Mean ± SE (pg Aβ/mg protein)
2-month-old	5	1.38 ± 0.24		0.20 ± 0.08	3.16 ± 1.44
12-month-old	5	11.51 ± 5.21	62.57 ± 17.68	4.77 ± 2.33	38.78 ± 4.97
17-month-old	8	81.08 ± 4.90	26005.61 ± 2391.14	6.60 ± 0.44	4465.46 ± 383.45
Ratios	Sol Aβ 1–40/1–42			Insol Aβ 1–40/1–42	
2-month-old	3.30 ± 0.87				
12-month-old	4.47 ± 2.42			1.51 ± 0.23	
17-month-old	12.64 ± 1.15			5.90 ± 0.41	

Table 2. Summary of hydrogen peroxide levels, carbonyl proteins and cytochrome *c* oxidase activity in Tg2576 and WT mice

	Mice studied	Hydrogen peroxide levels Mean ± SE	Difference/trend (nmol/mg mitochondrial protein)	Carbonyl proteins Mean ± SE	Difference/trend (pmol/mg mitochondrial protein)	Cytochrome oxidase activity Mean ± SE	Difference/trend (mU/mg mitochondrial protein)
2-month-old Tg2576 mice	5	5063.60 ± 626.36	1:0.75 = 25% increase in Tg2576 mice ($P < 0.01$)[a]	189.20 ± 19.76	1:0.8 = 20% increase in Tg2576 mice ($P = 0.38$)	0.13 ± 0.03	1:1.2 = 20% decrease in Tg2576 mice ($P = 0.58$)
2-month-old WT mice	5	3810.93 ± 619.41		152.75 ± 17.00		0.16 ± 0.03	
17-month-old Tg2576 mice	5	7519.00 ± 958.83	1:0.88 = 12% increase in Tg2576 mice ($P = 0.45$).	189.40 ± 18.26	1:1.07= No change	1.09 ± 0.17	1:0.77 = 23% increase in Tg2576 mice
17-month-old WT mice	5	6621.38 ± 613.88		202.50 ± 23.64		0.84 ± 0.09	

[a]Statistically significant.

Immunofluorescence analysis of 8-OHG in Tg2576 mice and WT mice

To determine the time course of oxidative damage, using immunohistochemical methods, we investigated cerebral cortex slices from 2- and 17-month-old Tg2576 mice and age-matched WT littermates. Our immunofluorescence analysis of 8-OHG revealed increased immunoreactivity in 17-month-old Tg2576 mice compared with the immunoreactivity found in 2-month-old Tg2576 mice, suggesting that oxidative damage in Tg2576 mice is dependent on the accumulation of mutant APP derivatives, including intraneuronal Aβ. We also observed increased immunoreactivity in the 17-month-old WT mice when compared with the immunoreactivity found in the 2-month-old WT mice, suggesting that aging is responsible for increased oxidative damage in the 17-month-old WT mice.

Hydrogen peroxide levels in brain mitochondria from Tg2576 mice and WT mice

To determine whether mutant APP and Aβ induce free radicals in mitochondria, we measured hydrogen peroxide levels in isolated mitochondria from 2- and 17-month-old Tg2576 mice and age-matched WT littermates. Tissues were not available or sufficient for 12-month-old Tg2576 mice and age-matched WT littermates. We found increased levels of hydrogen peroxide in both 2-month-old (25% increase with $P < 0.01$) and 17-month-old Tg2576 mice (12% increase, $P = 0.45$) when compared with the age-matched WT mice. However, the levels were statistically significant only in the 2-month-old Tg2576 mice ($P < 0.01$). We also observed an age-dependent increase of hydrogen peroxide in both the Tg2576 and WT mice (Table 2).

Carbonyl proteins in brain mitochondria from Tg2576 mice and WT mice

To determine whether Aβ alters carbonyl proteins in mitochondria, we measured carbonyl proteins in isolated mitochondria from 2- and 17-month-old Tg2576 mice and age-matched WT littermates. Tissues were not available or sufficient for 12-month-old Tg2576 mice and age-matched WT littermates. We found increased levels of carbonyl proteins in 2-month-old Tg2576 mice compared to the age-matched WT mice (20% increase, $P = 0.38$), but not in the 17-month-old Tg2576 mice. We also noticed an age-dependent increase of carbonyl proteins in both the Tg2576 and WT mice (Table 2).

Correlation of Aβ production and hydrogen peroxide levels and carbonyl proteins in Tg2576 mice and WT mice

As shown in Table 3, both soluble Aβ1–40 and Aβ1–42 directly correlated with hydrogen peroxide levels but not insoluble Aβ1–40 and Aβ1–42 in Tg2576 mice. Among soluble Aβ, we found statistically significant correlations only for soluble Aβ1–40 ($R = 0.71$ and $P = 0.02$; Table 3 and Fig. 7).

Table 3. Correlation of hydrogen peroxide and carbonyl proteins, with Aβ production in Tg2576 mice

	Sol Aβ1–40	Sol Aβ1–42	Insol Aβ1–40	Insol Aβ1–42
Hydrogen peroxide				
R	0.71	0.41	−0.09	0.42
P	0.02[a]	0.31	0.89	0.29
Number of mice	10	10	5	8
Carbonyl proteins				
R	0.1039	−0.14	0.67	0.14
P	0.78	0.75	0.23	0.74
Number of mice	10	10	5	8

[a]Statistically significant.

Cytochrome *c* oxidase activity in brain mitochondria from Tg2576 mice and WT mice

We found decreased levels of cytochrome *c* oxidase in 2-month-old Tg2576 mice (20% decrease, $P = 0.58$) compared with age-matched WT littermates. Tissues were not available or sufficient for 12-month-old Tg2576 mice and age-matched WT littermates (Table 2). However, we did not find a statistically significant decrease of cytochrome *c* oxidase activity in both the 2- and 17-month-old Tg2576 mice, compared with the age-matched WT mice (Table 2).

DISCUSSION

In the present study, using *in vivo* (Tg2576 mouse model) and *in vitro* (APP cell line), we found evidence demonstrating that both Aβ1–40 and Aβ1–42 are associated with brain mitochondria as the 4 kDa Aβ monomer (Figs 1 and 2). In addition to the 4 kDa Aβ monomer, we found that different sizes of oligomers are associated with mitochondria (Figs 4 and 5). Furthermore, our digitonin fractionation studies indicated that Aβ is more abundant in the mitoplast and less abundant in the outer membrane of mitochondria, suggesting that Aβ actually enters mitochondria (Fig. 6). These studies also suggest that Aβ interferes with mitochondrial function, with significantly increased hydrogen peroxide and carbonyls, and decreased cytochrome oxidase activity, particularly in the 2-month-old Tg2576 mice when compared with the age-matched WT littermates. The significant correlation found between hydrogen peroxide and soluble Aβ ($P < 0.01$) also supported the hypothesis that Aβ promotes mitochondrial dysfunction and oxidative damage.

Aβ and mitochondria

Oxidative damage in association with mitochondrial dysfunction has been reported in the AD literature. In late-onset, sporadic AD, an age-dependent increase of reactive oxygen species has been identified as a key factor in the development and progression of AD (12,20,24). In familial AD, mitochondrial oxidative damage has also been overwhelmingly documented (20). However, the precise mechanistic link between mitochondrial oxidative damage and abnormal APP processing has not been elucidated. In a previous global gene expression study of Tg2576 mice, we investigated the gene expression profiles of transcripts at three stages of disease progression (compared with age-matched WT littermates): long before (2 months), immediately before (5 months) and after (18 months) the appearance of Aβ plaque pathology and cognitive impairment (14). This analysis revealed that the genes related to mitochondrial energy metabolism and apoptosis were up-regulated in the 2-month-old Tg2576 mice compared with the age-matched WT mice and that the same genes were also up-regulated in the 5- and 18-month-old Tg2576 mice. These results suggest that mitochondrial energy metabolism may be impaired by the expression of mutant APP and/or Aβ, and that the up-regulation of mitochondrial genes may be a compensatory response (14).

In the present study, we found Aβ1–40 and Aβ1–42 in the mitochondrial membranes in both Tg2576 mice and N2a cells expressing the mutant human APP. Our immunoblotting analyses of mitochondrial pellets from N2a cells expressing human mutant APP cells demonstrated the presence of Aβ oligomers in mitochondrial membranes. However, we also found oligomer immunoreactivity in N2a cells over-expressing human WT APP cells, suggesting a possibility of oligomer formation in the absence of human APP mutation. Using human postmortem brains, several biochemical and electron microscopy studies revealed that the oligomers were observed as robust in AD subjects and as less abundant in non-demented subjects (38,39), supporting our present findings of oligomer formation in N2a cells over-expressing human WT APP cells.

Further, our digitonin fractionation studies showed that Aβ was more abundant in the inner mitochondrial membrane and matrix fractions and less abundant in the outer mitochondrial membrane. These novel findings suggest that mutant APP derivatives enter the mitochondria and possibly disrupt the ETC, ultimately leading to oxidative damage. This hypothesis is supported by recent findings from Crouch *et al*. (29) and Caspersen *et al*. (40), in which Aβ was localized in the mitochondria. For the first time, our study demonstrated that both monomeric and oligomeric forms of Aβ are associated with mitochondria in Tg2576 mice and in N2a cells expressing the human mutant APP.

The findings from the present study also support our findings from our gene expression study of Tg2576 mice (14), in which we found abnormal mitochondrial gene expressions and oxidative damage in 2-month-old Tg2576 mice but in which we rarely observed intraneuronal Aβ at this early stage of disease progression.

Taken together, these findings suggest a possible link between mutant APP and mitochondria. Although researchers have not found direct evidence of such an association, a previous study by Anandatheerthavarada *et al*. (41) demonstrated that mutant APP accumulates in mitochondrial membranes in Tg2576 mice. They found that a chimeric N-terminal signal in the APP molecule enters mitochondria, via positively charged residues of APP molecule at 40, 44 and 51, and results in the import of APP into the mitochondria. However, because of the presence of an acidic domain spanning residue 220–229 of the APP transmembrane arrest form occurs with C-terminal region of APP facing the cytosol. Thus, the orientation of APP associated with mitochondrial membranes is the N-terminus in intra-mitochondrial space and the C-terminus towards the cytosol. Such early import of APP into mitochondria may

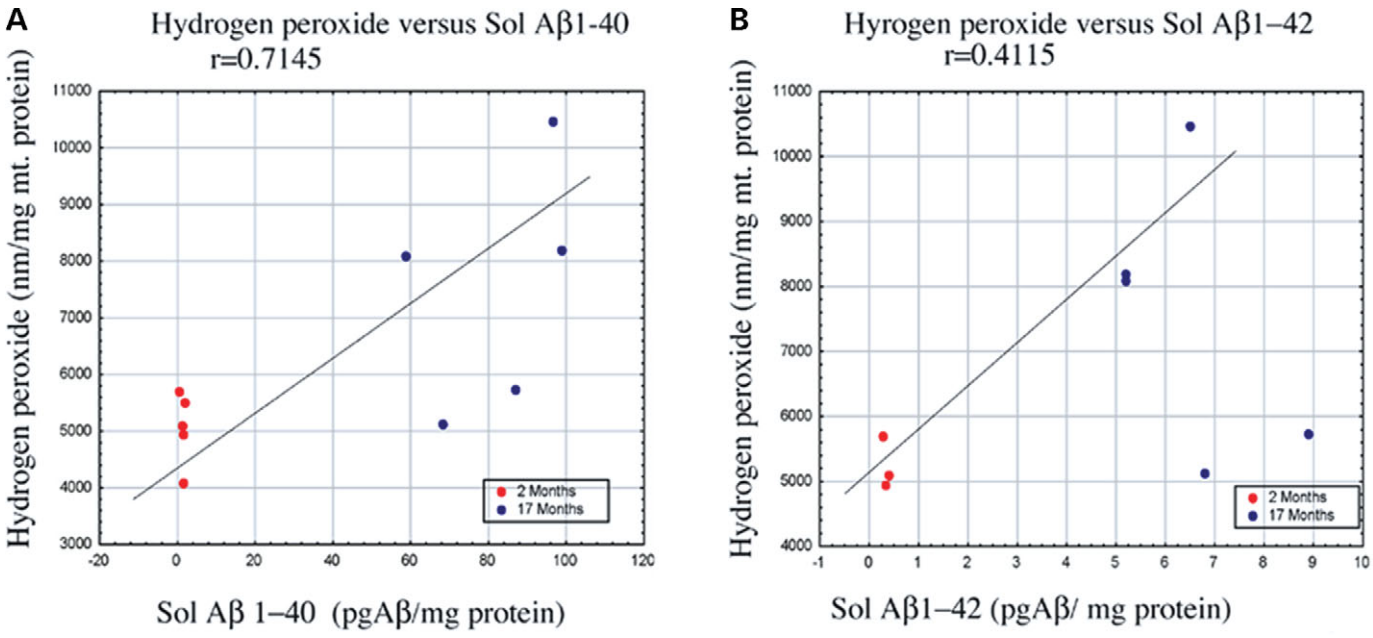

Figure 7. Correlative analysis of soluble Aβ and hydrogen peroxide production in Tg2576 mice. The *x*-axis represents soluble Aβ (in pg Aβ/mg protein), and the *y*-axis represents hydrogen peroxide levels (nm/mg mitochondrial protein). Image (**A**) is for soluble Aβ1–40 and image (**B**) for soluble Aβ1–42.

disrupt the ETC in Tg2576 mice and lead to oxidative damage, possibly because this early import (at least before a Tg2576 mouse turns 2 months of age), and the subsequent impairment in mitochondrial ETC, may lead to mitochondrial dysfunction in the 2-month-old Tg2576 mice. To compensate for the loss of mitochondrial function caused by mutant APP, mitochondrial genes may be activated in the early stages of disease progression in Tg2576 mice (14).

The accumulation of Aβ in mitochondria may be explained by two possible mechanisms: (1) If full-length APP molecules enter mitochondria, then cleavage of 40–42 residues of APP (or the 4 kDa Aβ peptide) might occur in the mitochondria because γ secretase activity has been present in mitochondria, and γ secretase is required to facilitate cleavage of the APP molecule (42). Otherwise, we cannot explain the presence of the γ secretase complex in the mitochondria, which has been established (42). (2) The cleavage of the APP molecule (via the activation of the γ secretase and BACE, another enzyme required for cleavage of the APP molecule) may occur primarily in the cytoplasm and in the cleaved 40–42 residues of Aβ that are later transported to mitochondria, but there is no experimental evidence to support this second possibility. Findings from the present study and others (40,41) suggest for the possible mechanism: that mutant APP and its derivatives enter mitochondria and generate free radicals, ultimately leading to oxidative damage. Further research is needed to determine the precise mechanism resulting in the transport of Aβ into the mitochondria in AD neurons.

Mutant APP and Aβ induces free radicals and oxidative DNA damage

Our present investigation of hydrogen peroxide radicals clearly suggests a relationship between the accumulation of mutant APP derivatives (Aβ monomers and oligomers) and hydrogen peroxide production in the mitochondria of Tg2576 mice but not in age-matched WT littermates. We found increased hydrogen peroxide levels, carbonyl proteins and decreased cytochrome oxidase activity in 2-month-old Tg2576 mice when compared with their age-matched WT littermates. These findings support our original hypothesis that mutant APP derivatives enter the mitochondria in early stages of disease progression and induce free radicals, leading to mitochondrial oxidative damage. Our study mainly focused on measuring hydrogen peroxide radicals, carbonyl proteins and cytochrome oxidase activity in the mitochondria, because mitochondria are a major source of free radicals, and it has been proposed that Aβ induces free radicals in the mitochondria (20,22,32,40).

As discussed earlier, in addition to intraneuronal Aβ, it is possible that mutant APP also induces free radicals after mutant APP enters mitochondria. It is unlikely that mutant APP derivatives can induce hydrogen peroxide radicals without affecting the mitochondria (26). Our previous findings of abnormal mitochondrial gene expressions in 2-month-old Tg2576 mice (14), biochemical studies of APP imported to mitochondria (41) and the present findings of increased hydrogen peroxide production in Tg2576 mice suggest that APP-mediated free radicals may be responsible for mitochondrial oxidative damage in Tg2576 mice. Our findings of oxidative damage in Tg2576 mice are in agreement with previous studies of oxidative stress in Tg2576 mice (9,10,22,34,59). A correlative analysis between soluble Aβ1–40, soluble Aβ1–42, insoluble Aβ1–40, insoluble Aβ1–42 and hydrogen peroxide production in Tg2576 mice revealed that only soluble Aβ1–40 and soluble Aβ1–42 directly correlated with hydrogen peroxide production but insoluble Aβ1–40 and insoluble Aβ1–42 did not (Table 3 and Fig. 7), further

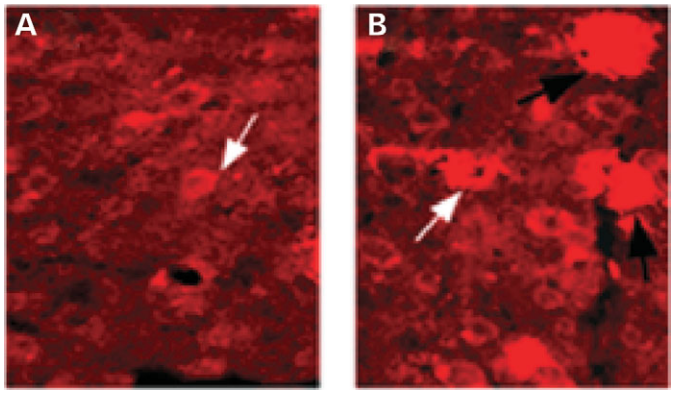

Figure 8. Aβ immunoreactivity in Tg2576 mice. A Tg2576 brain section immunostained with the Aβ1–42 antibody (labeled with Alexa 594). Intraneuronal Aβ was first found in the cortical neurons of 2-month-old Tg2576 mice (image **A**); later, both intraneuronal Aβ and extraneuronal Aβ were found abundantly in 17-month-old Tg2576 mice (image **B**). White arrows indicate intraneuronal Aβ and black arrows, extraneuronal Aβ or Aβ deposits.

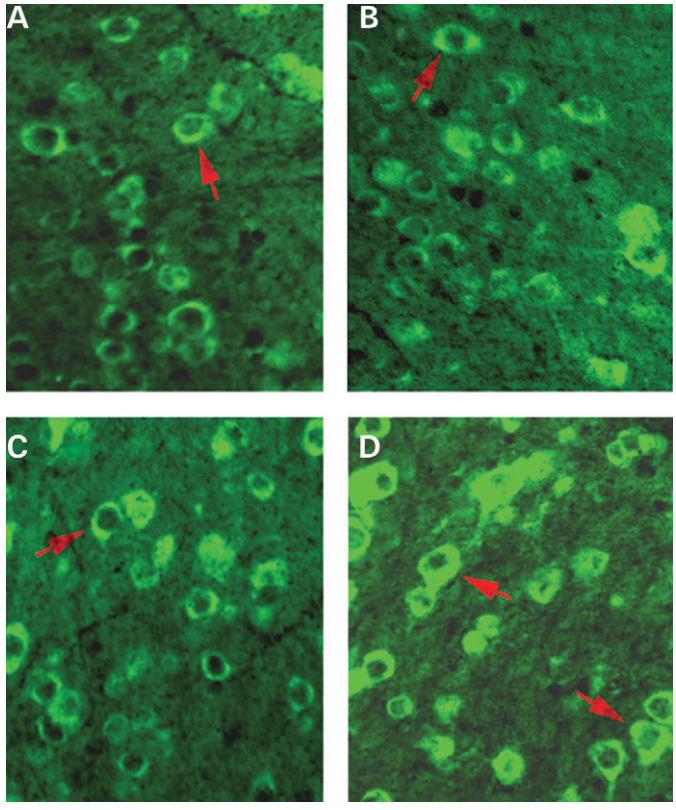

Figure 9. Immunoreactivity with the anti-8-OHG antibody in Tg2576 mice. (**A**) represents 2-month-old WT mice; (**B**) 2-month-old Tg2576 mice; (**C**) 17-month-old WT mice; and (**D**) 17-month-old Tg2576 mice. Increased levels of 8-OHG are shown in the cerebral cortex of 2- and 17-month-old Tg2576 mice compared with levels in the cerebral cortex of 2- and 17-month-old WT littermates. Arrows indicate increased immunoreactivity of 8-OHG.

strengthening support for our hypothesis that soluble Aβ enters mitochondria, induces free radicals and impairs mitochondrial metabolism in AD development and progression.

Findings from our immunofluorescence analysis of 8-OHG further support the presence of mitochondrial oxidative DNA damage in Tg2576 mice. We found DNA damage in 2-month-old Tg2576 mice and increases in DNA damage corresponding to the stages of disease development in Tg2576 mice (Fig. 9), suggesting that free radicals generated by mutant APP and its derivatives may likely be responsible for the mitochondrial oxidative DNA damage found in Tg2576 mice. However, to determine the precise connection between mitochondrial oxidative DNA damage and mutant APP derivatives in disease progression in Tg2576 mice from birth to death, quantitative methods such as HPLC are needed (43,44). Although apoptotic cell death has not been reported even in aged Tg2576 mice, mitochondrial oxidative DNA damage was evident in the study reported here and may be a key factor for synaptic dysfunction in Tg2576 mice.

It is now well established that mitochondrial oxidative DNA damage is a major factor in AD development and progression (9,11–14,45–48), and findings from this study and others support this hypothesis. In particular, using a comet assay, Migliore *et al*. (45) recently studied mitochondrial oxidative DNA damage in leukocytes in three subject groups: persons diagnosed with mild cognitive impairment (MCI), persons diagnosed with AD and healthy persons. Findings showed a significantly higher level of primary DNA damage in the leukocytes from the AD and the MCI subjects compared with the control subjects. Moreover, the amount of oxidized DNA bases (both purines and pyrimidines) was significantly higher in the MCI and AD subjects, compared with the amount of oxidized DNA bases in the control subjects, suggesting that oxidative stress, at least at the DNA level, may be an early event in the pathogenesis of AD (45). Such findings further support our results here. Further, in addition to DNA damage caused by mutant APP and Aβ that we observed, we also found increases in DNA damage corresponding to increases in the ages of the Tg2576 mice, supporting the widely accepted free-radical theory of aging in AD (21,22,44).

Our investigation here of carbonyl proteins showed that, in addition to mitochondrial oxidative DNA damage, increased oxidation of proteins occurred in 2-month-old Tg2576 mice. Although we did not find a statistically significant increase in carbonyl proteins in Tg2576 mice compared with the WT mice, our findings still indicate that proteins may gradually oxidize as the disease progresses. Further studies of carbonyl proteins in larger numbers of Tg2576 mice and age-matched WT littermates are needed to understand how Aβ is related to carbonyl proteins in the progression of AD. However, based on our study of carbonyl proteins, we suggest that oxidative damage may be an early event in AD progression. Oxidation of proteins is well documented in AD patients (49,50), and findings from this study support this observation.

Our investigation of Aβ production reported here revealed intraneuronal soluble Aβ in Tg2576 mice as young as 2-months old and that levels of both soluble and insoluble Aβ progressively increased in an age-dependent fashion (Table 1). The increase of soluble Aβ production significantly correlated with an increase of hydrogen peroxide radicals in Tg2576 mice. For other mitochondrial parameters, including

carbonyl proteins and cytochrome *c* oxidase, we found a trend in which there was a decrease in cytochrome *c* oxidase and an increase in carbonyl proteins, but these values were not statistically significant in Tg2576 mice. There are several possibilities for not finding statistical significance (Table 2) and not finding positive correlations with Aβ production (Table 3): (1) the sample size may have been too small in this study, (2) Aβ itself may act as free radical scavenger and may reduce mitochondrial oxidative damage (51) and (3) to reduce mitochondrial toxicity caused by mutant APP derivatives, other neuroprotective genes may be activated as AD progresses in Tg2576 mice (14,52). These issues can be resolved by extending the present study with a larger number of mice at each of the three different stages of disease progression (2, 12 and 24 months) in Tg2576 mice and age-matched WT mice.

Even with the non-statistical significance of a few mitochondrial parameters (carbonyl proteins and cytochrome *c* oxidase), the present statistically significant findings of increased hydrogen peroxide (Tables 1–3 and Figs 7–9) suggest that soluble Aβ may be responsible for the generation of hydrogen peroxide radicals, oxidative DNA damage and the carbonyl proteins in Tg2576 mice. As discussed earlier, if mutant APP derivates enter mitochondria, impair ETC and cause oxidative damage to AD neurons, then mitochondrially targeted antioxidants may effectively decrease free radicals and oxidative damage, and may protect AD neurons from mutant APP derivates (53). Our findings point to the possible development of mitochondrial therapies for AD, particularly antioxidants that target mitochondria.

CONCLUSIONS

The mechanistic link between abnormal mitochondrial gene expression and oxidative damage in AD development and progression is unclear. In the present study, using immunoblotting, digitonin fractionation, immunofluorescence and electron microscopy techniques, we studied relationships between mitochondria and Aβ in Tg2576 mice and N2a cells expressing mutant human APP and WT human APP. We found an association between mutant APP derivatives (Aβ monomers and oligomers) and mitochondria in cerebral cortex slices from Tg2576 mice and N2a cells expressing mutant APP. Further, to determine the functional relationship between mutant APP, Aβ and oxidative damage, we studied Tg2576 mice and age-matched WT littermates, quantifying Aβ levels, hydrogen peroxide levels, cytochrome *c* oxidase activity and carbonyl proteins. We found intraneuronal Aβ levels in Tg2576 mice as young as 2-months old, and an age-dependent increase in both soluble and insoluble Aβ levels in 12- and 17-month-old Tg2576 mice. In addition, we found a significant increase in hydrogen peroxide levels in Tg2576 mice compared with the age-matched WT littermates. This increase directly correlated with levels of soluble Aβ in Tg2576 mice, suggesting that soluble Aβ may be responsible for the production of hydrogen peroxide in Tg2576 mice. We found cytochrome *c* oxidase activity decreased in 2-month-old Tg2576 mice compared with age-matched WT littermates. However, further investigation of large numbers of Tg2576 mice and age-matched WT littermates—from birth to death—is needed to determine the precise link between cytochrome oxidase activity and mitochondrial Aβ. Further, interpreting how findings such as those reported here using a Tg2576 mouse model apply to persons with AD is a major challenge to mitochondrial and AD researchers, one that will require a time course study of Aβ production, free radical production and oxidative damage in the Tg2576 model. However, at this stage of AD research, we can say that findings from transgenic mouse models, including those from this study, suggest that the mechanism of oxidative damage may also apply to AD humans: that mutant APP and soluble Aβ may enter mitochondria, induce free radicals and impair mitochondrial metabolism.

MATERIALS AND METHODS

Mice

The Tg2576 mice and age-matched WT littermates were housed at the Neurological Sciences Institute of Oregon Health and Science University (OHSU) and at the Veteran Affairs Medical Center in Portland. The mice were a gift from Dr Karen Hsiao, University of Minnesota (54). The OHSU Institutional Animal Care and Use Committee approved all procedures for animal care according to guidelines set forth by NIH.

Cell lines

We used mouse N2a cells expressing either mutant human APP or WT human APP. The mutant and WT cell lines were a gift from Drs Sangram Sisodia and Gopal Thinakarn, University of Chicago (35). They were grown in a medium containing a 1:1 mixture of DMEM/10%FBS and OptiMEM, supplemented with 0.4 mg/Ml G418 (Invitrogen, CA, USA). After 48 h, the cells were harvested and used for immunoblotting analysis of Aβ.

Preparation of Tg2576 mice tissues and APP cells, and isolation of mitochondrial proteins

For tissue preparation, brains from Tg2576 mice and age-matched WT littermates were harvested. The mice were sacrificed by cervical dislocation, the brains were removed and cerebral cortices were dissected. Mitochondria were isolated from the cortex as described in Caspersen *et al*. (40), with modifications. Briefly, mouse tissues and/or mutant APP and WT cell lines were homogenized using a Teflon-glass homogenizer in 1:10 weight/volume of an ice-cold homogenization buffer (0.5 g/ml pepstatin, 0.5 g/ml leupeptin, 1 mM PMSF, 1 mM EDTA, 250 mM sucrose, 1 mM EGTA and 10 mM HEPES/NAOH; Percoll–final concentration 14%; pH 7.4). The protein lysates were centrifuged at 1500*g* for 10 min, and a supernatant mitochondrial pellet was collected. The bottom pellet was used as the 'nuclear pellet' for our immunoblotting analysis. A homogenization buffer with Percoll was added again to the nuclear pellet and centrifuged for 15 min at 9000*g* to pellet pure mitochondria. The nuclear pellet was resuspended in a wash buffer (0.5 g/

ml pepstatin 0.5 g/ml leupeptin, 1 mM PMSF, 250 mM sucrose, 1 mm EGTA, 1 mM EDTA and 10 mM Tris–HCl; pH 7.5) and centrifuged again. It was then resuspended in a wash buffer and stored at −80°C until the protein assay was performed. The concentration of mitochondrial proteins in each sample was determined using the BCA method (Pierce Biotechnology, Rockford, IL, USA).

Immunoblotting analysis of mitochondrial pellets from Tg2576 mice and APP cell lines

To detect the 4 kDa Aβ peptide in the mitochondrial pellet, 10 μg of the mitochondrial protein, which was prepared from Tg2576 and WT mice brain specimen and/or from APP and WT cell lines, was resolved on a 10–20% gradient gel (Tricine–SDS). To differentiate Aβ1–40 and Aβ1–42 residues in the mitochondrial pellet, a 4–20% gradient gel (Tricine–SDS) was used. The resolved protein was transferred to nylon membranes (Novax Inc., San Diego, CA, USA) that were then incubated at room temperature with a blocking buffer (5% dry milk dissolved in a TBST buffer) for 1 h. The nylon membranes were incubated with the primary antibodies Aβ1–40 (with a dilution of 1:100) and Aβ1–42 (1:100) (polyclonal rabbit) (Chemicon International, CA, USA), voltage-dependent anion channel (VDAC) (1:1500) and COX IV (1:1000) (monoclonal) (Molecular Probes, Eugene, OR, USA). The membranes were washed with a TBST buffer three times at 10 min intervals and then incubated with appropriate secondary antibodies for 2 h, followed by washing again three times with a TBST buffer. Protein expression was detected with chemiluminescent reagents (Pierce Biotechnology).

To determine whether oligomer formation of Aβ is associated with a mitochondrial fraction, both the nuclear and the mitochondrial pellets were resolved on a 10–20% gradient gel (Tricine–SDS). Immunoblotting analysis was performed using the A11-oligomer (polyclonal rabbit) antibody (1:1000) (Biosource International, CA, USA) that recognized only the oligomers (36) in our immunoblots.

Preparation of digitonin mitochondrial fractions and immunoblotting analysis

To separate mitochondrial membranes (outer, inner and matrix) from themitochondrial pellet prepared from APP cell lines, a digitonin fractionation method was used, following Schnaitman and Greenwalt (37). Briefly, a 2% digitonin stock solution was prepared. The BSA and digitonin were added to an ice-cold homogenization buffer (0.5 g/ml pepstatin, 0.5 g/ml leupeptin, 1 mM PMSF, 1 mM EDTA, 250 mM sucrose, 1 mM EGTA and 10 mM HEPES/NAOH; pH 7.4). An aliquot of the ice-cold buffer was added to the mitochondrial pellet through continuous stirring. The diluted suspension was homogenized gently by hand and centrifuged at 12 000*g*. The supernatant was carefully drawn off, and the pellet was gently resuspended in the isolation buffer. This suspension was centrifuged again at the same speed for 10 min. The pellet from the second centrifugation was designated as the 'low-speed pellet' or the 'inner-membrane plus matrix'. The supernatants from the first and second centrifugation were pooled and were designated as the 'low-speed supernatant'. The low-speed supernatant was fractionated at 144 000*g* for 1 h. The pellet from this centrifugation was designated as the 'high-speed pellet' or the 'outer membrane'. These low-speed and high-speed pellets were resolved in a 12% SDS-PAGE gel and used for immunoblotting analysis with Aβ1–40 (1:100) (polyclonal rabbit) (Chemicon International), and for analyses of mitochondrial antibodies COX IV (1:1000), ANT (1:1000) (inner membrane) (Molecular Probes), Mn-SOD (1:200) (matrix) (Sigma–Aldrich) and VDAC (1:1500) (outer membrane) (Molecular Probes).

Electron microscopy of the mitochondrial pellet

The isolated mitochondria from the Tg2576 mice and WT mice were fixed in a Karnovsky's fixative for 1 h and then rinsed in a 0.1 M sodium cacodylate buffer. They were post-fixed in 1% osmium tetroxide for 1 h, rinsed in water, dehydrated in a graded series of acetone and then infiltrated overnight in half acetone and half epon resin. The tissue was fixed in Epon 812 at 60°C for 12 h. The embedded blocks were sectioned on a Leica ultramicrotome. The sections were mounted on 300 mesh grids, stained with lead citrate and uranyl acetate, and viewed on a FEI Morgagni electron microscope. Images were captured with a 2K digital camera.

Measurement of hydrogen peroxide in isolated mitochondria

The production of hydrogen peroxide in the cortical mitochondria of Tg2576 mice and age-matched WT littermates was measured using an Amplex® Red Hydrogen Peroxide Assay Kit (A22188) (Molecular Probes). A BCA™ Protein Assay Kit (Pierce Biotechnology) was used to estimate the total mitochondrial proteins. The working reaction mixture contained the mitochondrial proteins (μg/μl), Amplex Red reagents (50 μM), horseradish peroxidase (HRP) (0.1 U/ml) and a reaction buffer (1X). The mixture was incubated at room temperature for 30 min before spectrophotometer readings were taken at 570 nm. Finally, hydrogen peroxide production was determined using a standard curve equation and were expressed in nmol/μg mitochondrial protein.

Measurement of cytochrome *c* oxidase activity in isolated mitochondria

Cytochrome *c* oxidase activity was measured in an isolated mitochondrial pellet. Enzyme activity was assayed spectrophotometrically using a Sigma Kit (Sigma–Aldrich) following manufacturer's instructions. Briefly, 2 μg of mitochondrial protein was added to 1.1 ml of the reaction solution, which contained 50 μl of 0.22 mM ferricytochrome *c* fully reduced by sodium hydrosulphide, Tris–HCl (pH 7.0) and 120 mM potassium chloride. The decrease of absorbance at 550 mM was recorded for a 1-min reaction at 10-s intervals, and cytochrome *c* oxidase activity of cytochrome oxidase was measured according to the following formula: mU/mg of total mitochondrial protein = (ΔA/min sample − (ΔA/min blank) × 1.1 mg protein × 21.84). The protein concentrations were determined following the BCA method.

Measurement of carbonyl proteins in isolated mitochondria

Carbonyl proteins in the cortical mitochondria of Tg2576 mice and age-matched WT littermates were determined with the Zentech PC Test (Protein Carbonyl Enzyme Immuno-Assay Kit; Biocell Corporation Ltd). Briefly, the mitochondrial samples (5 μl) were allowed to react with a dinitrophenylhydrazine (DNP) solution (200 μl). The DNP-reacted proteins bound non-specifically to an ELISA plate, and the unconjugated DNP and non-protein entities were washed away. The adsorbed DNP–protein was then probed with an anti-DNP-biotin antibody, followed by a streptavidin-linked HRP probe. Then the chromatin reagent that contained peroxide was added to catalyze the oxidation of TMB. Finally, the reaction was stopped by the addition of a stopping reagent (acid, provided with the kit), and the absorbance was measured for each well at 450 nm using a spectrophotometer. Along with controls and samples, protein carbonyl standards were also included in the assay. The content of the carbonyl protein in the mitochondrial samples was determined as pmol/mg protein, using the standard curve.

Measurement of soluble and insoluble Aβ levels inTg2576 mice and WT mice

The cerebral cortex from the right half of each mouse brain was snap-frozen on dry ice at the time of sacrifice and stored at −70°C until a homogenate was prepared according to Lim *et al*. (55) and Stackman *et al*. (56). Briefly, samples were homogenized in a Tris-buffered saline (pH 8.0) containing protease inhibitors (20 mg/ml pepstatin A, aprotinin, phophsoramidon and leupeptin; 0.5 mM PMSF; and 1 mM EGTA). Samples were sonicated briefly and centrifuged at 10 000*g* for 20 min at 4°C. The soluble fraction was used to determine the soluble Aβ by ELISA. To measure the insoluble Aβ, the pellet was re-suspended in 70% formic acid and again centrifuged. The extract was neutralized with 0.25 M Tris (pH 8.0) containing 30% acetonitrile and 5 M NaOH before we used ELISA to determine the insoluble Aβ. For each sample, Aβ1–40 and Aβ1–42 were measured using commercial colorimetric ELISA kits (Biosource International) specific for each species. A 96-well plate washer and reader were used, following the manufacturer's instructions. Each sample was run in duplicate. The protein concentrations of the homogenates were determined by the BSA method, and Aβ was expressed as pg Aβ/mg protein.

Immunofluorescence analysis of oxidative damage in Tg2576 mice and WT mice

To determine whether oxidative damage occurs early in AD progression, we studied 8-OHG in brain specimens from 2-month-old ($n = 5$), 8-month-old ($n = 5$) and 17-month-old Tg2576 mice ($n = 5$); and from 2-month-old ($n = 5$), 8-month-old ($n = 5$) and 18-month-old WT mice ($n = 5$). Immunofluorescence was carried out following Reddy *et al*. (14) and Manczak *et al*. (44). The sections were blocked with a buffer solution (0.5% Triton in PBS +10% rabbit serum +1% BSA) and then incubated overnight at room temperature with a goat anti-8-OHG, polyclonal antibody (1:50 dilution) (Alpha Diagnostics, San Antonio, TX, USA). On the day after primary antibody incubation, the sections were washed with a washing buffer (0.5% Triton in PBS). For 8-OHG, the sections were incubated with a secondary biotinylated anti-mouse antibody at a dilution of 1:2000 (Vector Laboratories, Burlingame, CA, USA) for 1 h at room temperature. The sections were then washed with PBS (pH 7.4) three times for 10 min each and were blocked for 1 h with a 1% blocking buffer (Molecular Probes). They were subsequently incubated with a streptavidin HRP solution for 1 h (Molecular Probes) and then washed with PBS (pH 7.4) three times for 10 min each. The sections were treated with the fluorescent dye Alexa 488 (green) (Molecular Probes) for 10 min at room temperature and counter-stained with Hoechst (1:1000) (blue) for nuclear labeling. Photographs were taken with a multiphoton laser scanning microscope system (Zeiss Meta LSM510).

Immunofluorescence analysis of intraneuronal Aβ and Aβ deposits in Tg2576 mice

We used immunofluorescence analysis to determine the expression of intraneuronal Aβ and Aβ deposits in Tg2576 mice in 2, 8- and 17-month-old Tg2576 mice, following Reddy *et al*. (14) and Manczak *et al*. (44). Briefly, the brain sections were fixed in 4% paraformaldehyde and incubated overnight at room temperature, with rabbit anti-Aβ1–42 polyclonal antibody in a 1:100 dilution (Chemicon International). On the next day, the sections were incubated with the secondary antibody anti-mouse HRP in a 1:200 dilution for 1 h. Then the slides were incubated with the tyramide-tagged fluorescent dye Alexa 594 (red) (Molecular Probes) for 10 min at room temperature. Photographs were taken with a multiphoton laser scanning microscope system (Zeiss Meta LSM510).

Statistical analysis

Descriptive statistical analysis was carried out for Aβ production (only in Tg2576 mice), hydrogen peroxide, carbonyl proteins and cytochrome *c* oxidase activity in Tg2576 mice and age-matched WT littermates. To determine relationships between Aβ production and hydrogen peroxide levels, and Aβ production and carbonyl proteins, if any, we conducted correlation analyses.

SUPPLEMENTARY MATERIAL

Supplementary material is available at HMG Online.

ACKNOWLEDGEMENTS

The authors thank Sandra Oster, OHSU Neurological Sciences Institute, for critical reading of the manuscript. This research was supported in part by the American Federation for Aging Research (to P.H.R.), the U.S. Department of Veteran's Affairs Advanced Research Career Development Award and NIH-AT0006 (to J.Q.) and NCRR grant no. RR016858.

Conflict of Interest statement. Authors declare that they have no conflict of interest regarding this manuscript.

REFERENCES

1. Selkoe, D.J. (2001) Alzheimer's disease: genes, proteins, and therapy. *Physiol. Rev.*, **81**, 741–766.
2. Mattson, M.P. (2004) Pathways towards and away from Alzheimer's disease. *Nature*, **430**, 631–639.
3. Tanzi, R.E. and Bertram, L. (2005) 20 years of the Alzheimer's disease amyloid hypothesis: a genetic perspective. *Cell*, **120**, 545–555.
4. Reddy, P.H. and McWeeney, S. (2005) Mapping cellular transcriptosomes in autopsied Alzheimer's disease subjects and relevant animal models. *Neurobiol. Aging*, Published online ahead of print September 9.
5. Walsh, D.M., Klyubin, I., Fadeeva, J.V., Cullen, W.K., Anwyl, R., Wolfe, M.S., Rowan, M.J. and Selkoe, D.J. (2002) tNaturally secreted oligomers of amyloid beta protein potently inhibit hippocampal long-term potentiation *in vivo*. *Nature*, **416**, 535–539.
6. Hardy, J. and Selkoe, D.J. (2002) The amyloid hypothesis of Alzheimer's disease: progress and problems on the road to therapeutics. *Science*, **297**, 353–356.
7. Sisodia, S.S., Annaert, W., Kim, S.H. and De Strooper, B. (2001) Gamma-secretase: never more enigmatic. *Trends Neurosci.*, **24** (Suppl. 11), S2–S6.
8. Pappolla, M.A., Omar, R.A., Kim, K.S. and Robakis, N.K. (1992) Immunohistochemical evidence of oxidative [corrected] stress in Alzheimer's disease.. *Am. J. Pathol.*, **140**, 621–628. Erratum in *Am. J. Pathol.*, (1996) **149**, 1770.
9. Bozner, P., Grishko, V., LeDoux, S.P., Wilson, G.L., Chyan, Y.C. and Pappolla, M.A. (1997) The amyloid beta protein induces oxidative damage of mitochondrial DNA. *J. Neuropathol. Exp. Neurol.*, **56**, 1356–1362.
10. Pappolla, M.A., Chyan, Y.J., Omar, R.A., Hsiao, K., Perry, G., Smith, M.A. and Bozner, P. (1998) Evidence of oxidative stress and *in vivo* neurotoxicity of beta-amyloid in a transgenic mouse model of Alzheimer's disease: a chronic oxidative paradigm for testing antioxidant therapies *in vivo*. *Am. J. Pathol.*, **152**, 871–877.
11. Hirai, K., Aliev, G., Nunomura, A., Fujioka, H., Russell, R.L., Atwood, C.S., Johnson, A.B., Kress, Y., Vinters, H.V., Tabaton, M. *et al*. (2001) Mitochondrial abnormalities in Alzheimer's disease. *J. Neurosci.*, **21**, 3017–3023.
12. Swerdlow, R.H. and Khan, S.M. (2004) A 'mitochondrial cascade hypothesis' for sporadic Alzheimer's disease. *Med. Hypotheses*, **63**, 8–20.
13. Manczak, M., Park, B.S., Jung, Y. and Reddy, P.H. (2004) Differential expression of oxidative phosphorylation genes in patients with Alzheimer's disease: implications for early mitochondrial dysfunction and oxidative damage. *Neuromolecular Med.*, **5**, 147–162.
14. Reddy, P.H., McWeeney, S., Park, B.S., Manczak, M., Gutala, R.V., Partovi, D., Jung, Y., Yau, V., Searles, R., Mori, M. and Quinn, J. (2004) Gene expression profiles of transcripts in amyloid precursor protein transgenic mice: up-regulation of mitochondrial metabolism and apoptotic genes is an early cellular change in Alzheimer's disease. *Hum. Mol. Genet.*, **13**, 1225–1240.
15. Reddy, P.H., Mani, G., Park, B.S., Jacques, J., Murdoch, G., Whetsell, W., Jr., Kaye, J. and Manczak, M. (2005) Differential loss of synaptic proteins in Alzheimer's disease: implications for synaptic dysfunction. *J. Alzheimers Dis.*, **7**, 103–117.
16. Kitazawa, M., Oddo, S., Yamasaki, T.R., Green, K.N. and LaFerla, F.M. (2005) Lipopolysaccharide-induced inflammation exacerbates tau pathology by a cyclin-dependent kinase 5-mediated pathway in a transgenic model of Alzheimer's disease. *J. Neurosci.*, **25**, 8843–8853.
17. Tanzi, R.E. (2005) The synaptic Abeta hypothesis of Alzheimer disease. *Nat. Neurosci.*, **8**, 977–979.
18. Oddo, S., Caccamo, A., Tran, L., Lambert, M.P., Glabe, C.G., Klein, W.L. and Laferla, F.M. (2006) Temporal profile of amyloid-beta (Abeta) oligomerization in an *in vivo* model of Alzheimer disease: a link between Abeta and Tau pathology. *J. Biol. Chem.*, **281**, 1599–1604.
19. Butterfield, D.A., Drake, J., Pocernich, C. and Castegna, A. (2001) Evidence of oxidative damage in Alzheimer's disease brain: central role for amyloid beta-peptide. *Trends Mol. Med.*, **7**, 548–554.
20. Reddy, P.H. and Beal, M.F. (2005) Are mitochondria critical in the pathogenesis of Alzheimer's disease? *Brain Res. Brain Res. Rev.*, **49**, 618–632.
21. Beal, M.F. (2005) Mitochondria take center stage in aging and neurodegeneration. *Ann. Neurol.*, **58**, 495–505.
22. Reddy, P.H. (2006) Amyloid precursor protein-mediated free radicals and oxidative damage: implications for the development and progression of Alzheimer's disease. *J. Neurochem.*, **96**, 1–13.
23. Swerdlow, R.H., Parks, J.K., Cassarino, D.S., Maguire, D.J., Maguire, R.S., Bennett, J.P., Jr., Davis, R.E. and Parker, W.D., Jr. (1997) Cybrids in Alzheimer's disease: a cellular model of the disease? Neurology, **49**, 918–925.
24. Khan, S.M., Cassarino, D.S., Abramova, N.N., Keeney, P.M., Borland, M.K., Trimmer, P.A., Krebs, C.T., Bennett, J.C., Parks, J.K., Swerdlow, R.H., Parker, W.D., Jr. and Bennett, J.P., Jr. (2000) Alzheimer's disease cybrids replicate beta-amyloid abnormalities through cell death pathways. *Ann. Neurol.*, **48**, 148–155.
25. Casley, C.S., Canevari, L., Land, J.M., Clark, J.B. and Sharpe, M.A. (2002) Beta-amyloid inhibits integrated mitochondrial respiration and key enzyme activities. *J. Neurochem.*, **80**, 91–100.
26. Cardoso, S.M., Santos, S., Swerdlow, R.H. and Oliveira, C.R. (2001) Functional mitochondria are required for amyloid beta-mediated neurotoxicity. *FASEB J.*, **15**, 1439–1441.
27. Cardoso, S.M., Santana, I., Swerdlow, R.H. and Oliveira, C.R. (2004) Mitochondria dysfunction of Alzheimer's disease cybrids enhances Abeta toxicity. *J. Neurochem.*, **89**, 1417–1426.
28. Keil, U., Bonert, A., Marques, C.A., Scherping, I., Weyermann, J., Strosznajder, J.B., Muller-Spahn, F., Haass, C., Czech, C., Pradier, L., Muller, W.E. and Eckert, A. (2004) Amyloid beta-induced changes in nitric oxide production and mitochondrial activity lead to apoptosis. *J. Biol. Chem.*, **279**, 50310–50320.
29. Crouch, P.J., Blake, R., Duce, J.A., Ciccotosto, G.D., Li, Q.X., Barnham, K.J., Curtain, C.C., Cherny, R.A., Cappai, R., Dyrks, T., Masters, C.L. and Trounce, I.A. (2005) Copper-dependent inhibition of human cytochrome *c* oxidase by a dimeric conformer of amyloid-beta 1–42. *J. Neurosci.*, **25**, 672–679.
30. Aleardi, A.M., Benard, G., Augereau, O., Malgat, M., Talbot, J.C., Mazat, J.P., Letellier, T., Dachary-Prigent, J., Solaini, G.C. and Rossignol, R. (2005) Gradual alteration of mitochondrial structure and function by beta-amyloids: importance of membrane viscosity changes, energy deprivation, reactive oxygen species production, and cytochrome *c* release. *J. Bioenerg. Biomembr.*, **37**, 207–225.
31. Abdul, H.M., Sultana, R., Keller, J.N., Clair, D.K.S., Markesbery, W.R. and Butterfield, D.A. (2006) Mutations in amyloid precursor protein and presenilin-1 genes increase the basal oxidative stress in murine neuronal cells and lead to increased sensitivity to oxidative stress mediated by amyloid b-peptide (1–42), H_2O_2 and kainic acid: implications for Alzheimer's disease. *J. Neurochem.*, **96**, 1322–1335.
32. Lustbader, J.W., Cirilli, M., Lin, C., Xu, H.W., Takuma, K., Wang, N., Caspersen, C., Chen, X., Pollak, S., Chaney, M. *et al*. (2004) ABAD directly links Abeta to mitochondrial toxicity in Alzheimer's disease. *Science*, **304**, 448–452.
33. Smith, M.A., Perry, G., Richey, P.L., Sayre, L.M., Anderson, V.E., Beal, M.F. and Kowall, N. (1996) Oxidative damage in Alzheimer's. *Nature*, **382**, 120–121.
34. Pratico, D., Uryu, K., Leight, S., Trojanoswki, J.Q. and Lee, V.M. (2001) Increased lipid peroxidation precedes amyloid plaque formation in an animal model of Alzheimer amyloidosis. *J. Neurosci.*, **21**, 4183–4187.
35. Thinakaran, G., Teplow, D.B., Siman, R., Greenberg, B. and Sisodia, S.S. (1996) Metabolism of the 'Swedish' amyloid precursor protein variant in neuro2a (N2a) cells. Evidence that cleavage at the 'beta-secretase' site occurs in the golgi apparatus. *J. Biol. Chem.*, **271**, 9390–9397.
36. Kayed, R., Head, E., Thompson, J.L., McIntire, T.M., Milton, S.C., Cotman, C.W. and Glabe, C.G. (2003) Common structure of soluble amyloid oligomers implies common mechanism of athogenesis. *Science*, **300**, 486–489.
37. Schnaitman, C. and Greenawalt, J.W. (1968) Enzymatic properties of the inner and outer membranes of rat liver mitochondria. *J. Cell Biol.*, **38**, 158–175.
38. Kuo, Y.M., Emmerling, M.R., Vigo-Pelfrey, C., Kasunic, T.C., Kirkpatrick, J.B., Murdoch, G.H., Ball, M.J. and Roher, A.E. (1996) Water-soluble Abeta (N-40, N-42) oligomers in normal and Alzheimer disease brains. *J. Biol. Chem.*, **271**, 4077–4081.

39. Kokubo, H., Kayed, R., Glabe, C.G. and Yamaguchi, H. (2005) Soluble Abeta oligomers ultrastructurally localize to cell processes and might be related to synaptic dysfunction in Alzheimer's disease brain. *Brain Res.*, **1031**, 222–228.
40. Caspersen, C., Wang, N., Yao, J., Sosunov, A., Chen, X., Lustbader, J.W., Xu, H.W., Stern, D., McKhann, G. and Yan, S.D. (2005) Mitochondrial Abeta: a potential focal point for neuronal metabolic dysfunction in Alzheimer's disease. *FASEB J.*, **19**, 2040–2021.
41. Anandatheerthavarada, H.K., Biswas, G., Robin, M.A. and Avadhani, N.G. (2003) Mitochondrial targeting and a novel transmembrane arrest of Alzheimer's amyloid precursor protein impairs mitochondrial function in neuronal cells. *J. Cell Biol.*, **161**, 41–54.
42. Hansson, C.A., Frykman, S., Farmery, M.R., Tjernberg, L.O., Nilsberth, C., Pursglove, S.E., Ito, A., Winblad, B., Cowburn, R.F., Thyberg, J. and Ankarcrona, M. (2004) Nicastrin, presenilin, APH-1 and PEN-2 form active gamma-secretase complexes in mitochondria. *J. Biol. Chem.*, **279**, 51654–55160.
43. Helbock, H.J., Beckman, K.B., Shigenaga, M.K., Walter, P.B., Woodall, A.A., Yeo, H.C. and Ames, B.N. (1998) DNA oxidation matters: the HPLC-electrochemical detection assay of 8-oxo-deoxyguanosine and 8-oxo-guanine. *Proc. Natl Acad. Sci. USA*, **95**, 288–293.
44. Manczak, M., Jung, Y., Park, B.S., Partovi, D. and Reddy, P.H. (2005) Time-course of mitochondrial gene expressions in mice brains: implications for mitochondrial dysfunction, oxidative damage, and cytochrome *c* in aging. *J. Neurochem.*, **92**, 494–504.
45. Migliore, L., Fontana, I., Colognato, R., Coppede, F., Siciliano, G. and Murri, L. (2005) Searching for the role and the most suitable biomarkers of oxidative stress in Alzheimer's disease and in other neurodegenerative diseases. *Neurobiol. Aging*, **26**, 587–595.
46. Pratico, D. (2005) Peripheral biomarkers of oxidative damage in Alzheimer's disease: the road ahead. *Neurobiol. Aging*, **26**, 581–583.
47. Gibson, G.E. and Huang, H.M. (2005) Oxidative stress in Alzheimer's disease. *Neurobiol. Aging*, **26**, 575–578.
48. Beal, M.F. (2005) Oxidative damage as an early marker of Alzheimer's disease and mild cognitive impairment. *Neurobiol. Aging*, **26**, 585–586.
49. Korolainen, M.A., Goldsteins, G., Nyman, T.A., Alafuzoff, I., Koistinaho, J. and Pirttila, T. (2006) Oxidative modification of proteins in the frontal cortex of Alzheimer's disease brain. *Neurobiol. Aging*, **27**, 42–53.
50. Boyd-Kimball, D., Castegna, A., Sultana, R., Poon, H.F., Petroze, R., Lynn, B.C., Klein, J.B. and Butterfield, D.A. (2005) Proteomic identification of proteins oxidized by Abeta(1–42) in synaptosomes: implications for Alzheimer's disease. *Brain Res.*, **1044**, 206–215.
51. Bush, A.I., Atwood, C.S., Goldstein, L.E., Huang, X. and Rogers, J. (2000) Could Abeta and AbetaPP be antioxidants? *J. Alzheimers Dis.*, **2**, 83–84.
52. Stein, T.D. and Johnson, J.A. (2002) Lack of neurodegeneration in transgenic mice overexpressing mutant amyloid precursor protein is associated with increased levels of transthyretin and the activation of cell survival pathways. *J. Neurosci.*, **22**, 7380–7388.
53. Reddy, P.H. Mitochondrial oxidative damage in Aging and Alzheimer's Disease: implications to mitochondrially targeted antioxidants. *J. Biomed. Biotech.*, in press.
54. Hsiao, K., Chapman, P., Nilsen, S., Eckman, C., Harigaya, Y., Younkin, S., Yang, F. and Cole, G. (1996) Correlative memory deficits, Abeta elevation, and amyloid plaques in transgenic mice. *Science*, **274**, 99–102.
55. Lim, G.P., Chu, T., Yang, F., Beech, W., Frautschy, S.A. and Cole, G.M. (2001) The curry spice curcumin reduces oxidative damage and amyloid pathology in an Alzheimer transgenic mouse. *J. Neurosci.*, **21**, 8370–8387.
56. Stackman, R.W., Eckenstein, F., Frei, B., Kulhanek, D., Nowlin, J. and Quinn, J.F. (2003) Prevention of age-related spatial memory deficits in a transgenic mouse model of Alzheimer's disease by chronic Ginkgo biloba treatment. *Exp. Neurol.*, **184**, 510–520.
57. Bijur, G.N. and Jope, R.S. (2003) Rapid accumulation of Akt in mitochondria following phosphatidylinositol 3-kinase activation. *J. Neurochem.*, **87**, 1427–1435.
58. McEnery, M.W., Dawson, T.M., Verma, A., Gurley, D., Colombini, M. and Snyder, S.H. (1993) Mitochondrial voltage-dependent anion channel. Immunochemical and immunohistochemical characterization in rat brain. *J. Biol. Chem.*, **268**, 23289–23296.
59. Smith, M.A., Hirai, K., Hsiao, K., Pappolla, M.A., Harris, P.L., Siedlak, S.L., Tabaton, M. and Perry, G. (1998) Amyloid-beta deposition in Alzheimer transgenic mice is associated with oxidative stress. *J. Neurochem.*, **70**, 2212–2215.